

Chapter 6

Redox potential and protonation pattern of the native and artificial cytochrome b

The redox active proteins contain redox centers. These can be organic or metal compounds and complexes, which are important for their function. The redox potentials of the cofactors represent key parameters of these proteins. In chapter 3, I described the way how we generated the structure of the artificial Cb from scratch. Then, we used that structure to evaluate the redox potentials of its two hemes. In this chapter, I discuss the results on the redox potentials of the artificial Cb and analyze the factors of the protein environment that determine the redox potentials of the two hemes. After that, I will discuss the results on the redox potentials of the native Cb in the mitochondrial Cbc₁ complex of bovine heart to validate the procedure of calculating the redox potentials of the hemes in proteins of known X-ray structure, to test the set of charges that we used in these applications and to compare these results with available experimental data.

6.1 Methods

6.1.1 *Computation of the heme redox potentials and protonation and redox patterns in proteins*

The protonation states of the protonatable residues and the oxidation states of the redox-active groups (hemes) were determined simultaneously by calculating the electrostatic energies, solving the linearized Poisson-Boltzmann equation (LPBE) numerically on a grid with finite difference method and using subsequent a Monte Carlo (MC) titration technique. The redox potentials of the hemes in the native and artificial Cb were evaluated by averaging over all sampled protonation and redox states of the titratable groups. All four considered hemes, from the native and artificial Cb are b-type hemes (protoporphyrin IX) with two histidines axially coordinated to the iron. Although all these hemes are of the same chemical nature, their redox potentials differ, since they are placed in a different protein environment. The basic theoretical problem in calculating the pK_a and redox potential values is to predict how the protein environment shifts these values of the variably charged groups in the protein from that of the isolated amino acid or heme in solution. Assuming that electrostatic interactions play the main role in tuning pK_a and redox potentials in the proteins, the differences of the redox potentials are caused by different interactions with other charged and polar groups of the protein and by different solvent accessibilities of the hemes. Because the protonatable groups contribute also to the redox potential differences due to the mutual interactions with hemes, the redox potential of the hemes depends also on pH.

The electrostatic energy of titratable groups in the protein environment is calculated relative to suitable model systems, which serve as a reference. The model compounds of titratable amino acid side chains are the corresponding isolated amino acids in aqueous

solution where the N- and C-termini are acetylated and amidated, respectively. For the redox potential of the heme, we used as reference system the bis-histidinyl heme model compound in aqueous solution, where the experimental value of the redox potential is -220 mV (Wilson, 1983). The method assumes that the difference in the titration behavior of an ionizable group in a protein and in a model compound can be accounted for by calculating the difference in the electrostatic work of altering the charges from the unprotonated to the protonated state in the protein and the work of making the same alteration in the model compound. The electrostatic potential is assumed to be given by the LPBE in which the protein interior has a low dielectric value ($\epsilon_p = 4$) (for the choice of this value see: Honig and Nicholls, 1995; Rabenstein et al., 1998b; Warshel et al., 1997), the solvent has a high dielectric value ($\epsilon_s = 80$), and the counterion (Boltzmann) terms are excluded from a region near the protein surface. By using the finite difference method to solve the LPBE, we are able to take into account the detailed shape of the protein surface as defined by the atomic coordinates of the protein, and the charge distribution given by the atomic partial charges. The PB calculations were carried out using the program MULTIFLEX from the MEAD (Macroscopic Electrostatics with Atomic Detail) suite of programs (Bashford & Gerwert, 1992; Bashford, 1997). First, it computes the electrostatic potentials for each titratable group in aqueous solution and in the protein, for protonated (oxidized) and deprotonated (reduced) form. Further, from the electrostatic potentials, the Born solvation energy term, the energy term of the interactions with background charges and the energy of the coupling between each pair of variably charged sites are calculated. The first two terms together with the $pK_{\text{mod},\mu}$ value of the proper model compound (see Appendix D) contribute to the intrinsic $pK_{\text{int},\mu}$ value, while the interaction energies between the charged titratable sites are elements of the so called W-matrix. The mobile ions in a solvent were modeled by ionic strength of 100 mM. An ion exclusion layer of 2 Å and a solvent probe radius of 1.4 Å were used. To solve the LPBE, a grid focusing procedure was used with decreasing grid spacing.

The computation of the electrostatic energies G_n (eq. 2.47) for the different charge patterns n of a protein and subsequent Monte Carlo titration was done with the program KARLSBERG. The number of titratable groups in artificial and native Cb, is too large for a direct evaluation of the Boltzmann averaged sums (2.48). Therefore, we used a Monte Carlo (MC) titration method, incorporated in program KARLSBERG (Rabenstein, 1999; Rabenstein & Knapp, 2001), to sample the protonation and redox states of the protein and to evaluate the protonation and oxidation probabilities of titratable groups at different pH and E_{sol} values. To improve the sampling efficiency of the MC titration, also two (three) titratable groups that couple stronger than 2.5 (5.0) pK_a units change their protonation state simultaneously in one MC move. Such double and triple moves were done in addition to simple moves. Each MC scan consists of at least of N simple MC moves, where it is attempted to change the protonation state of one titratable group. For each MC titration, we performed 1000 full MC scans and after that 10000 reduced scans, where all titratable groups that did not change their protonation state after first 1000 MC scans were fixed in their respective protonation state and excluded from further sampling. This MC titration procedure led to a standard deviation of less than 0.01 protons at each titratable group. We applied such a complete sampling procedure for each pH value varying from 0 to 14 in steps of 0.1 pH units, at 300 K and a solution redox potential of $E_{\text{sol}} = 0$ mV, what corresponds to an acid-base titration. For the artificial Cb, we performed redox titrations, at pH range from 5 to 9 and 300 K, changing the solution redox potential E_{sol} with a 20 mV increment in the range from -400 to $+300$ mV. An redox titration was done for each step of 0.2 pH units in the pH range between 5 and 9. Accordingly, in this application we considered for the artificial Cb the definitions of the $pK_a(pH, E_{\text{sol}}=0)$ and $E_{\mu}^0(pH, E_{\text{sol}}=0)$ (see eq. 2.50 and 2.51), as well as, the $pK_{1/2,\mu}$ and $E_{1/2,\mu}$.

6.1.2 Titratable groups

The C-termini, the N-termini, the heme propionates, aspartates, glutamates, arginines, lysines, cysteines, tyrosines and histidines, with the exception of the histidines coordinated to hemes, were considered as titratable groups, regardless whether they were involved in a salt bridge or not. The two hemes (H_I and H_{II}) of the native as well as artificial Cb together with the corresponding axially ligated imidazoles were considered as redox-active sites. Therefore, each heme contributes with three variably charged groups (one redox-active site and two PR groups). Each non-ligating histidine is represented by two titratable groups. Namely, there are two hydrogen atoms (ϵ -H and δ -H) at the imidazole ring that can get deprotonated. Both forms were considered in our calculation (Bashford et al., 1993) by representing them as two strongly coupled titratable sites, which cannot simultaneously be deprotonated. The Cbc₁ complex contains two additional cofactors. These are the heme of the cytochrome c₁ (Cc₁) subunit and the iron-sulfur cluster from the Rieske (ISP) subunit. Both were considered to be in the reduced form, because their redox potentials are too high. Furthermore, since the heme of the Cc₁ subunit is more than 35 Å away from the closest heme (H_I) of the Cb subunit, the solvent exposed PR groups of the Cc₁ heme were considered as non-titratable and were fixed in their unprotonated state.

6.1.3 Atomic partial charges

Most of the charges that we used in this application have been used successfully before to calculate redox potentials of cofactors (Rabenstein et al., 1998a,b; Rabenstein et al., 2000), or the protonation patterns in proteins (Vagedes et al., 2000; Rabenstein & Knapp, 2001). All additional charges needed in this application were computed with procedures that we used in similar applications before. The atomic partial charges of the amino acids including the protonated and deprotonated states of the titratable amino acids, were taken from the CHARMM22 (MacKerell et al., 1998) parameter set. But for some of the titratable residues (Arg, Cys, Lys, Tyr, C-ter, N-ter) charges were available for the standard protonation state only. For these residues, the atomic partial charges were calculated with the program SPARTAN using the semi-empirical PM3 method and the CHELPG procedure (Breneman & Wiberg, 1990), where the charges are determined such that they reproduce the electrostatic potential outside of the considered molecular group appropriately. For the iron sulfur cluster, the charges were taken from Izrailev et al., 1999. The heme was divided into three parts, where the porphyrin system and the PR groups were treated as independent titratable groups that interact electrostatically only. Thereby, the porphyrin moiety of the heme with the two axially ligated imidazoles is considered to be the redox-active site. For the atomic partial charges of the propionic acid, the same charges were used as for the side chain of glutamate taken from the CHARMM22 parameter set. The electronic wave functions of different redox states of the bis-imidazole heme model compound were calculated with the Hartree-Fock method from GAUSSIAN98 (Frisch et al., 1998) using the 6-31G* basis set for the iron atom and STO-3G basis set for all other atoms. The atomic partial charges were obtained from the wave functions of the quantum chemical computations by adjusting the electrostatic potential in the neighborhood of the heme with the Merz-Kollman approach (Besler et al, 1990).

To reduce the number of independent atomic partial charges, which have to be determined, we constrained the charges of hydrogen atoms bound at CH₂ or CH₃ groups to be equal, except for the hydrogens at the CAA and CAD carbon atoms, where we fixed the charges of two hydrogens at 0.09 and of one at 0.00. In the complete heme, the neutral hydrogen is replaced by the charge neutral CH₂ group of the propionic acid. Also the charge

of the hydrogen atom at the axially ligated imidazole ring that will be replaced later by the $C_{\beta}H_2$ group was constrained to be 0.09, since it is the total charge of that group. In similar applications, one can get the negative charge for metal atom. Even so, a charge set with a negative charge at the iron atom gives practically the same results for the electrostatic energies and the redox potentials (Rabenstein et al., 1998a,b; Rabenstein et al., 2000), we preferred to avoid a negative charge at the heme iron and fixed the charge of the iron to be +0.48 and +0.25 for oxidized and reduced bis-histidinyl heme, respectively. These charges, as well as the dipole and quadrupole moments were constrained, using the program RESP (Restrained ElectroStatic Potential) from Kollman. RESP fits the quantum mechanically calculated electrostatic potential at molecular surfaces using an atom-centered point charge model (Bayly et al., 1993; Cornell et al., 1993). A specially useful feature of this program is the possibility to constrain partial atomic charges of some atoms and to calculate a charge distribution of a molecule, keeping the dipole and quadrupole moment constant. The partial atomic charges and calculated redox potentials depend on the orientation of the ligated imidazole rings and on the heme conformation (Popović et al., unpublished data). Therefore, we performed the quantum chemical computation for all four conformations of the heme model compounds (two for the native and two for the artificial Cb). With this method, the atomic partial charges were calculated to represent the electrostatic potential faithfully in the neighborhood of the heme model compound. The atomic partial charges of the bis-histidinyl heme model compound and for all other titratable residues are given Appendix E.

6.1.4 Preparation of structures for electrostatic computations

The electrostatic calculations of the native Cb was done using the X-ray structure (PDB code 1BE3, Iwata et al., 1998) of the bovine heart Cbc₁ complex, consisting of 11 subunits. The three common subunits of Cb, Cyt c₁ and Rieske iron-sulfur protein are among them. The hydrogen atom coordinates were generated with the HBUILD command of CHARMM22, leading to an all atom representation of the Cbc₁ complex. Subsequently, the hydrogen atom positions were energetically minimized, keeping all other atoms fixed.

For calculations using only the Cb subunit, we took the C chain of the Cbc₁ complex. It consists of 379 residues and two hemes with a total number of 6242 atoms. It possesses 79 titratable groups, including the hemes, propionates and histidines. To solve the LPBE for that system, a two-step grid focusing procedure was applied, starting with a cubic lattice of 151 Å length and 1.0 Å grid spacing, followed by a 22.75 Å cube with 0.25 Å grid spacing. The whole Cbc₁ complex contains 2030 residues, three hemes and one iron-sulfur cluster with a total of 31996 atoms. We considered 661 variably charged sites as protonatable or redox active. The LPBE for the whole Cbc₁ complex was solved using a three-step grid focusing, starting from a 302 Å cube lattice with a grid spacing of 2.0 Å, followed by a 101 Å cube with 1.0 Å grid spacing and finally a 25.25 Å cube with a grid spacing of 0.25 Å. The lattices of lower resolution were centered with respect to the geometric center of the protein. The lattices with highest resolution were centered at the considered titratable groups.

In comparison, the artificial Cb contains 122 residues and two hemes, with a total number of 2218 atoms. The 52 titratable amino acids, two redox-active hemes and four PR groups, give a total of 58 variably charged groups. To solve the LPBE for the artificial Cb, a two-step grid focusing was performed, starting with cubic lattice of 105 Å with 1.0 Å grid spacing, followed by a 22.75 Å cube with 0.25 Å grid spacing.

6.2 Results and discussion

6.2.1 Calculations on the artificial cytochrome b

6.2.1.1 Protonation pattern of titratable groups

Since, the protonation and redox states of the titratable groups depend on each other, for a given pH and solution redox potential E_{sol} , the ensemble of protonation and redox patterns had to be calculated simultaneously by a statistical averaging method employed in a MC program. Most of the titratable groups, at pH = 7 and a solution redox potential of $E_{\text{sol}} = 0$ mV, are in the standard protonation state. Only Arg5(F₁) and the propionate PRA(H_h) exhibit deviations from standard protonation behavior (see Fig. 6.1). Their protonation probabilities at pH = 7 and $E_{\text{sol}} = 0$ mV, are 0.916 and 0.654, respectively. The propionate PRA(H_h) has a higher $pK_{a1/2}$ value than PRA(H_l) and starts to get deprotonated just below pH = 6. This may be due to the salt bridge of PRA(H_h) with Arg5(F₁), which is slightly "weaker" (more distant) than the corresponding salt bridge involving PRA(H_l), and due to the interaction of the positively charged Lys23(G₁) and Lys23(G₂), which are close to PRA(H_h) and may weaken its salt bridge. These two Lys could possibly be responsible what Arg5(F₁) starts to deprotonate already at pH=6.5. In the pH range of 7 to 12, Arg5(F₁) exhibits a non-monotonous titration behavior. In the same pH range the titration curve of PRA(H_h) exhibits a plateau. Both is probably due to a strong electrostatic interaction between Arg5(F₁) and PRA(H_h), which are involved in a salt bridge. They are situated in the more hydrophobic core of the four-helix bundle, what also may have an influence on their mutual interactions.

At neutral pH, the charges of four arginines and four propionates, as well as, the charges of lysines and glutamates cancel each other. Nevertheless, the total charge of the model protein is +2, due to the charges of the two oxidized hemes. Therefore, the pI value (isoelectric point), that corresponds to zero charge of a protein, is shifted towards higher pH values (pI= 9.3). Monitoring the pH dependence of the total charge of the artificial Cb (not shown), one can clearly distinguish titration in two steps, where the acidic groups titrate at pH around 4, and basic groups at pH about 11.

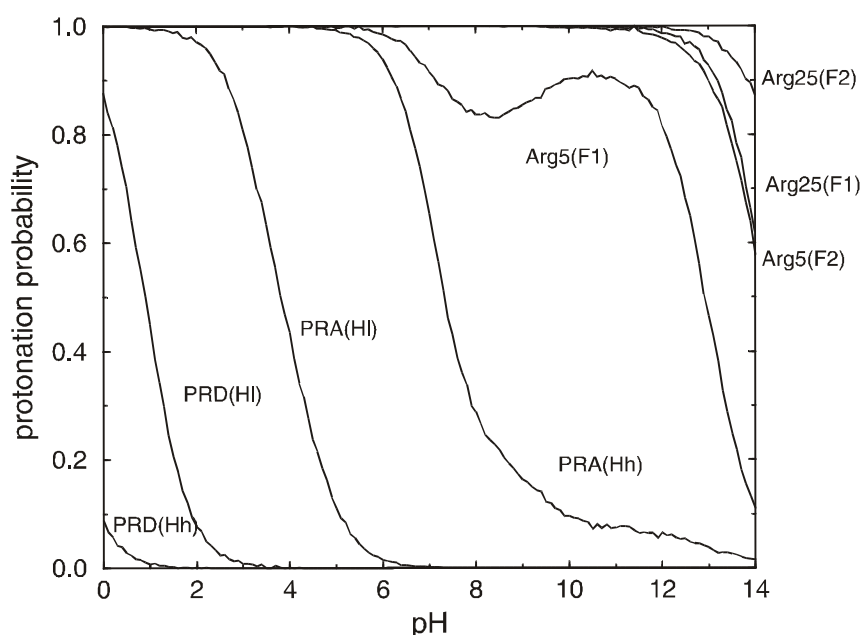


Figure 6.1: Titration curves of arginines and heme propionates in the artificial Cb at $E_{\text{sol}} = 0$ mV. The PR groups are denoted according to the pyrrole ring of heme where they are attached to (A or D) and the heme where they belong to (high- H_h or low- H_l potential heme). The arginines Arg5(F₁), Arg5(F₂), Arg25(F₁), and Arg25(F₂) form salt bridges with PRA(H_h), PRD(H_h), PRA(H_l), and PRD(H_l), respectively. The corresponding O–H distances between the PR groups and the arginines are 2.4 Å, 1.6 Å, 2.1 Å, and 1.5 Å.

6.2.1.2 *Experimental values of redox potentials*

The redox potential of the hemes in the artificial Cb at $T = 293$ K, $\text{pH} = 7$ and $I = 100$ mM, was determined by redox potentiometry. The redox titration curve was obtained by plotting the difference of the absorbance at the α -band (560nm) of the reduced minus that of the fully oxidized species against the ambient redox potential in the range between +50 and -300 mV (Rau & Haehnel, 1998). The data for the titration in reductive and oxidative direction exhibit two distinct midpotentials of -106 mV and -170 mV with standard deviation of ± 8 mV. These values are significantly higher than the midpotential of -220 mV of a synthetic four-helix bundle which accommodates one bis-histidine ligated heme (Choma et al., 1994) and the midpotential of -215 mV of an imidazole-histidine ligated single heme octapeptide (Harbury et al., 1965). In line with these values are also the potentials of -205 and -215 mV of the two non-interacting hemes of the four-helix bundle cytochromes of Robertson et al., (1994). These synthetic four-helix bundles consist of a single polypeptide chain, which can not efficiently protect the hemes from the solvent. Hence, the values around -220 mV seem to be typical for bis-histidine ligated hemes in a hydrophilic protein environment and without arginines to form salt bridges with the PR groups. The redox potential of the isolated heme with axially ligated imidazoles in solution was also measured to be -220 mV (Wilson, 1983). The structure of Haehnel's synthetic Cb is characterized by close packing of the four-helix bundle around the hemes, better shielding against the solvent and strong electrostatic interactions of the heme PR groups with four arginines. All of that results in higher values of the redox potential of the hemes. In comparison with the native complexes, the closest values of the heme redox potential are -50 mV and -170 mV (Kramer and Crofts, 1994a,b) found for the two hemes in the cytochrome b_6f (Cb_6f) complex. The two hemes in the Cb subunit of the Cbc_1 complex from bovine heart have with +93 mV and -34 mV at $\text{pH} = 7$ (Nelson & Gellerfors, 1974, 1975) more positive values of the redox potential. Although the design of the heme binding core was adopted to be very close to the Cb-subunit of the Cbc_1 complex, there are significant differences in the wavelength of maximum absorbance and in the redox potential of the hemes in the native and artificial Cb.

In the native Cb, H_h and H_l refer to the hemes with high and low redox potentials, which would correspond to the positions of the hemes near the open end and the template, respectively, when the orientation of the helices is used as reference (Rau & Haehnel, 1998). However, the heme near the template is better shielded from the solvent and should therefore possess a higher value of the redox potential than the one at the open end. A reliable assignment of the high and low potential heme in the artificial Cb was possible by orienting the four-helix bundle with the open ends of the two G helices fixed at a gold electrode and observing the voltage dependence of the current of the ET from the gold electrode to the artificial Cb hemes in a time resolved experiment (Willner et al., 1999). By this method, the redox potentials of the two hemes close to the open end and close to the template were measured to be -188 mV and -118 mV, respectively. Hence, with respect to the helix orientation, the high and low potential hemes in the artificial Cb are exchanged relative to the native Cb. Our computations will show to what extent a distinct heme environment and the electrostatic interaction between two almost identical hemes cause the difference in the redox potentials.

6.2.1.3 *Calculated heme redox potentials*

Using the calculated oxidation probabilities and expression (2.51), we evaluated the redox potential of the hemes. The experimental and theoretically calculated redox potentials at $\text{pH} = 7$ and $E_{\text{sol}} = 0$ mV are given in Table 6.1. The obtained values of -91 mV for the heme near to the template and -167 mV for the heme near to the open end of the four-helix bundle agree

very well with measured values of the artificial Cb in solution, which are -106 mV and -170 mV (Rau & Haehnel, 1998). However, they differ from the values -118 mV and -188 mV, obtained for the artificial Cb attached to a gold electrode (Willner et al., 1999). These discrepancies are presumably due to the different dielectric boundary.

The different arrangement of the substituents ($-\text{CH}_3$ and $-\text{CH}=\text{CH}_2$) at the pyrrole rings B and C, breaks a mirror symmetry of the heme (see Fig. 4.1). Consequently, there are two possibilities for the mutual orientation of the hemes in the artificial Cb. We consider for most of our computations the orientation of the hemes, which corresponds to that found in the native Cb ("native" conformation). Since there is no experimental evidence that only this conformation is assumed in the artificial Cb, we computed also the redox potentials for the alternative conformation obtained by rotating one of the hemes by 180° around the CHA–CHC axis. We refer to that orientation as "non-native" conformation of the hemes. The corresponding redox potentials (-90 and -162 mV) exhibit only minor changes, as one can see from the Table 6.1. This is not surprising, since both substituents are non-polar and there are only small changes in the structure by rotating the heme.

The pH dependence of the heme redox potentials in the artificial Cb is displayed in Fig. 6.2A. The redox potential of the heme is a pH dependent due to the electrostatic coupling with the protonation reactions at the titratable residues of the protein. The stronger the coupling, the more the redox potential decreases with an increase of the pH. From figure 6.2A, one can see that heme H_h exhibits a stronger pH dependence than the heme H_l . The residues, that are strongly coupled with redox-active part of the hemes, and that at the same time change their charge state are responsible for the different behavior of the two hemes. In this model structure, those residues are the four arginines and the corresponding PR groups involved in salt bridges. As we will see later on, buried salt bridges have a stronger influence on the redox potential than solvent exposed ones, where the interactions are screened by the high dielectric constant of water. Accordingly, the redox potential of H_h heme decreases by 18 mV/pH, while it remains practically constant for H_l heme at pH values between 6 and 9. At lower pH values the redox potential of that heme becomes also pH dependent, since its PR groups start to get deprotonated and change their charge state.

6.2.1.4 Role of the Phe and Trp and the electrostatic coupling of the hemes

The two phenylalanines Phe15(F_1) and Phe15(F_2) are situated in the middle of the four-helix bundle between the two hemes. Their role in shielding the heme redox potentials can be tested by replacing them by two alanines. The resulting shifts in the redox potentials $+4$ and -8 mV for H_h and H_l , respectively, are pretty small. Hence, the cavities with a dielectric constant of $\epsilon = 80$ created by removing the phenyl rings have a similar effect on the redox potentials as the phenyl rings. However, the phenyl rings may serve to mediate the ET between the two hemes. The influence of the phenylalanine side chain charges on the redox potential of the two hemes were investigated by setting them to zero. The obtained shifts in redox potentials are $+1$ and -5 mV for high and low potential heme, respectively. It demonstrates that the phenylalanine side chain charges practically do not have any influence. Since the phenylalanine is a non-polar and hydrophobic residue, it can influence the redox potential by its low dielectric constant rather than by the atomic charges themselves.

The two tryptophans in the structure of the artificial Cb are supposed to shield the low potential heme on the open end of the four helix-bundle from the solvent. However, the tryptophans can not protect the heme H_l near the open end of the four-helix bundle so efficiently as does the template with the heme H_h . Hence, the solvent accessibility of the two hemes differs and it is a main reason for the difference in their redox potentials. Similar as for the phenylalanines, the influence of the tryptophan side chain charges on the redox potential

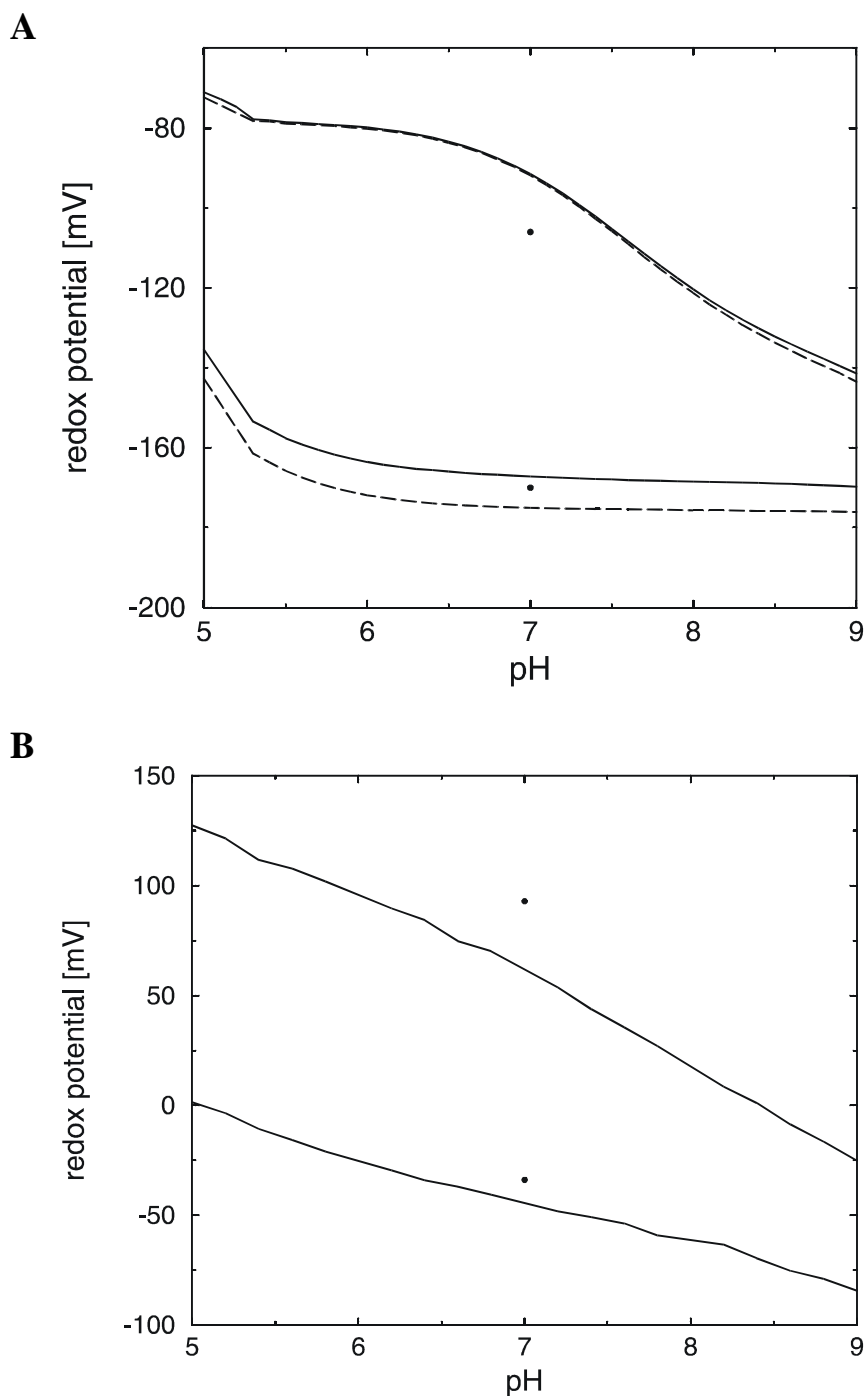


Figure 6.2: (A) pH dependence of the redox potential of the two hemes in the artificial Cb. The experimental values are given by the dots. The pH dependence of the redox potential of the two hemes is displayed in the physiological relevant pH regime from 5 to 9. The redox potentials were evaluated as $E_{\mu}^0(pH, E_{sol}=0 \text{ mV})$ (solid lines) according to eq. (2.51) and as $E_{1/2,\mu}$ value (dashed lines), see Chapter 2 for more details. Upper curves provide data for the high potential heme H_h close to the template, lower curves for the low potential heme H_l near the open end of the four helix-bundle. (B) pH dependence of the redox potential of the two hemes in the native Cb subunit. The experimental values are given by the dots. The pH dependence of the redox potentials of the two hemes is displayed in the physiological relevant pH regime from 5 to 9. The redox potentials were evaluated as $E_{\mu}^0(pH, E_{sol}=0 \text{ mV})$.

of the hemes is relatively small (0 and +11 mV), since tryptophan is a non-polar residue with rather small atomic charges. Hence, they act rather by changing the dielectric boundaries of the protein system.

It is also of interest to investigate to what extent the couplings of the redox states of the two hemes can influence each other. For that purpose, we considered only one of the two hemes is redox-active, while the other remains in its reduced uncharged redox state. However, the calculated difference in the redox potentials between the coupled and uncoupled hemes is less than 10 mV (see Table 6.1). The shortest distance between the two hemes is 14.9 Å (Fe–Fe distance is 21.6 Å) and what is probably more important their PR groups are oriented opposite to each other. Experimental data also suggest a small coupling between the two hemes.

6.2.1.5 Influence of dielectric medium and specific charge distribution

In Table 6.1, the third column gives the average shift of the redox potential of the two hemes relative to the value of –220 mV that is the redox potential of an isolated bis-histidine heme in aqueous solution. The average shift of the redox potential of the two hemes relative to the value in aqueous solution is:

$$\Delta E_{\text{sol}} = \frac{1}{2} [E(\text{H}_1) + E(\text{H}_h)] - E_{\text{sol}} \quad (6.1)$$

The fourth column displays the influence of setting specific atomic charges of the synthetic Cb to zero on the difference of the redox potentials of the two hemes. Both relative contributions are also given as percentage in brackets in Table 6.1.

To get a rough idea about the influence of the atomic charges on the redox potential of the hemes, we set the charges of all residues in the artificial Cb to zero. The obtained potentials of the two hemes become very similar and their values are shifted toward the value of –220 mV in aqueous solution. However, even after removing all atomic charges, the redox potentials of the H_h and H_l hemes are 42 and 38 mV more positive than the solution redox potential of the heme. The redox potential of the heme H_l near the open end is slightly closer to the solution value than the redox potential of the heme H_h, which is close to the template and therefore better shielded from the solvent. Since, inside of the four-helix bundle is still left the low dielectric medium, using the eq. 6.1, we estimated this contribution to be about 44% of the total shift of $\Delta E_{\text{sol}}(\text{total}) = 91$ mV. The remaining 56% of the overall shift is due to the specific charge distribution in the artificial Cb.

Removing the atomic charges of the protein backbone, the difference in the redox potentials of the two hemes remains almost the same. However, the redox potentials of both hemes become more negative, such that the backbone charges contribute about 52% (the complement of 48%) to the total average shift relative to the solution value of the redox potential. Going in opposite direction from the zero backbone charges toward the charges which the backbone atoms assume in the structure of the artificial Cb, the heme redox potentials increase for about 48 mV on the average. Hence, the backbone dipoles generate a positive potential in this model protein. Because the backbone has zero net charge, the non-zero potential is unexpected. In a recent study, Gunner et al. (2000) have shown that the asymmetry in packing the peptide amide dipole results on the average in more positive than negative electrostatic potential inside proteins of all folding motifs. An explanation is that the backbone dipoles with their CO groups are more likely to be surface exposed and amine protons prefer to be buried. Hence, the reduce form of redox-active groups is stabilized by a positive potential of the backbone dipoles, what increases the redox potential of the cofactors.

Table 6.1. Redox potentials of hemes in artificial Cb in mV at pH = 7 and $E_{\text{sol}} = 0$ mV.

experimental values:	heme, H_h near template	heme, H_l near open end	average shift^a	difference
Rau & Haehnel, 1998 ^b	-106	-170	+82	+64
Willner et al., 1999	-118	-188	+67	+70
bis-histidine ligated heme in solution	-220	-220	0	0
computed values:				
full model with native heme conformation ^c	-91	-167	+91	+76
full model with non-native heme conformation ^c	-90	-162	+94	+72
full model with uncoupled hemes ^d	-100	-176	+82	+76
contributions from different parts by setting atomic charges to zero for:				
all residues	-178	-182	+40 (44) ^e	+4 (5) ^f
backbone	-142	-211	+43.5 (48)	+69 (90)
template with links ^g	-95	-167	+89 (98)	+72 (95)
inner hydrophobic ^h side chains	-101	-168	+85.5 (94)	+67 (88)
outer hydrophilic ^h side chains	-92	-129	+109.5 (120)	+37 (49)
all four Arg and PR ⁱ	-140	-178	+61 (67)	+38 (50)

^a Average shift of the redox potentials relative to the solution value according to eq. (6.1).

^b The assignment of the measured high and low redox potentials to the two hemes was not certain from the original experiment (Rau & Haehnel, 1998). In the table the assignment was made in agreement with more recent experiments (Willner et al., 1999) and the present computational results.

^c The native heme conformation corresponds to the relative orientation of the hemes as it is in the native Cb, where the hemes can be matched after two 180° rotations, one around the virtual bond CHA-CHC and a second around CHB-CHD. Omitting the second rotation operation corresponds to the non-native heme conformation. For more informations, see point A4 of the generation of atomic coordinates in Appendix I. If not otherwise stated the native heme conformation is used.

^d The redox states of the two hemes are uncoupled by calculating the electrostatic energies for the redox state of one heme by fixing the redox state of the other heme in the uncharged reduced state.

^e Fraction in % of the calculated average shift of redox potentials referring to the calculated value of 91 mV.

^f Fraction in % of the calculated difference of redox potentials referring to the calculated value of 76 mV.

^g The links to the template involve the residues Gly1(F₁), Gly1(F₂) and Lys27(G₁), Lys27(G₂).

^h The inner hydrophobic and outer hydrophilic side chains are defined as in figure 5.3, but excluding the arginines and histidines.

ⁱ The four arginines, which form salt bridges with the PR groups of the hemes, are Arg5(F₁), Arg5(F₂) and Arg25(F₁), Arg25(F₂).

The influence of the atomic charges of the template on the redox potentials of the hemes can be probed by setting these charges to zero. No significant change in redox potentials is observed (see Table 6.1), since the template does not contain polar or titratable groups. The template has only a weak (4 mV) direct influence on the redox potential of the H_h heme, but indirectly it shields very strongly the H_h heme from the influence of the water. An additional electrostatic computation shows that the difference of redox potentials disappears very much (−151 vs. −168 mV for the H_h and H_l hemes, respectively) by removing the coordinates of all atoms from template and connecting residues. The redox potential of the H_h heme shifts by 60 mV toward the corresponding value of −220 mV for the heme in aqueous solution. Hence, the template with its dielectric boundaries and dielectric constant of 4, makes the corresponding environment around the H_h heme more hydrophobic and the heme H_h less solvent accessible. Buried hemes prefer to be in the reduced state and generally have higher values of the redox potential, than water exposed hemes.

6.2.1.6 Influence of different residues on the redox potentials

Next, we considered the effect of different residue types on the shift of the redox potentials. Turning off all atomic charges of the hydrophobic side chains in the interior of the four-helix bundle has only a small effect on the shift of the redox potentials. This is not surprising, since the corresponding charges are small. Practically, only the H_h heme is effected by these charge changes, what can indicate that it is somewhat better packed in the hydrophobic pocket than H_l heme. The influence of charges of the hydrophobic residues on the difference in the redox potential of the two hemes is also small (12%).

On the other hand, turning off the atomic charges of the charged and polar side chains on the outer solvent exposed surface of the four-helix bundle (excluding the arginines and the axially ligated histidines, which are anyhow inside of the binding pocket) has a large effect. The charges of the hydrophilic side chains practically do not have any effect on the high potential heme H_h at the better shielded closed end of the four helix-bundle, whereas the redox potential of the low potential heme shifts by 38 mV to higher values. It means that for the H_l heme, negatively charged glutamates exhibit a stronger effect on the redox potential than positively charged lysines. The effects from glutamates and lysines seem to cancel each other for the H_h heme. Consequently, the charges of the hydrophilic side chains contribute more than 50% to the difference of the redox potentials. At the same time, these charges exhibit a mild but negative contribution of 20% to the shift of the average redox potential.

Finally, we consider the influence of the salt bridges between the PR groups of the hemes and the arginines Arg5 and Arg25 of the two *F* helices. Setting the corresponding atomic charges to zero, we obtained the redox potentials of −140 and −178 mV for the heme near the template and near the open end, respectively (Table 6.1). Accordingly, the charges of the four salt bridges with their corresponding molecular groups contribute about 50% to the difference in the redox potentials of the two hemes and 33% to the overall shift of the redox potentials relative to the solution value. The salt bridges of the PR groups with the arginines give rise to a much stronger shift of the redox potential for the heme near the template (H_h) than for the heme close to the open end (H_l). That is not surprising, since buried salt bridges are generally stronger than solvent exposed salt bridges.

Notice that the different contributions do not add up exactly to 100%, since these electrostatic energies are not exactly additive.

6.2.2 Calculations on the native cytochrome b

Accuracy of the atomic coordinates and the reliable set of the atomic charges are crucial for the electrostatic computations. Since no crystal structure is available for the artificial Cb, the atomic coordinates were obtained by a modeling procedure, whose quality can not directly be assessed. In conventional applications, the atomic coordinates are taken from a crystal structure. Good agreement between the calculated and experimental measured redox potentials for the computer-generated structure of the artificial Cb has motivated us to test our computational procedure and set of partial atomic charges that we used, also with the crystal structure of a native bis-histidine heme protein. Therefore, we performed the same computations on the Cbc1 complex of bovine heart (Iwata et al., 1998), obtained at pH = 6.6 at 3.0 Å resolution.

6.2.2.1 Protonation pattern of titratable groups

In the native Cb subunit, at pH = 7 and $E_{\text{sol}} = 0$ mV, the following residues are in non-standard protonation state (protonation probability is given in brackets): Asp254 (0.39), Asp331 (1.00), Glu162 (0.24), Glu202 (0.06), Glu271 (0.99), Lys227 (0.68), N-terminus (0.045), PRA(H_i) (0.045), PRD(H_i) (0.96), PRA(H_h) (0.64) and PRD(H_h) (0.32). From eight histidine residues in the Cb subunit only for three (Hi68, His201 and His345) the fraction of the double protonated form is somewhat larger 0.75, 0.10 and 0.10, respectively. All other histidines are neutral, with a proton residing on the δ - or ϵ -nitrogen. The number of titratable groups in the whole bc₁ complex, which possess non-standard protonation is of course much larger. Interestingly, Glu271 is very close to the H_i heme (the shortest distance is 3.4 Å) and close to the propionic group PRA of the H_i heme (5.4 Å away from the O1A atom). Since, Glu271 is situated in a hydrophobic pocket formed by Pro270, Phe128, Phe274 but in the neighborhood of the negatively charged PRA(H_i) group, it is completely protonated.

In the physiological pH range between 6 to 8 and a solvent redox potential of $E_{\text{sol}} = 0$ mV, the high potential heme (H_h) is in the reduced and the low potential heme (H_i) is in the oxidized state. At the same time, looking at the titration curves of the heme propionates, we noticed that the propionic groups of the H_h heme are symmetrically protonated and exhibit only a mild pH dependence, whereas the protonation pattern of the propionates of the H_i heme is asymmetric. Namely, PRD(H_i) is almost protonated, while PRA(H_i) is nearly deprotonated. This behavior can be explained by the salt bridges formed between the PR groups and arginines and by additional interactions with the local protein environment. Arg80 forms a strong salt bridge with PRA(H_i) (O–H distance 2.08 Å), and only a weak salt bridge (O–H distance 3.8 Å) with the second PR group (PRD(H_i)) at the same heme. Furthermore, the later PR group is surrounded by several hydrophobic residues (Leu51, Tyr55, Val66 and Pro134) and does not form an H-bond. The PR group PRA(H_h) from heme H_h also forms a strong salt bridge with Arg100 (O–H distance 1.99 Å) and a weak salt bridge (O–H distance 3.2 Å) with the other propionate PRD(H_h). But, in contrast to the corresponding PRD(H_i) group, the PRD group of heme H_h is in addition to the salt bridge also involved in two H-bonds with the amide hydrogen of Asn206 (O–H distance 1.90 Å), and the hydroxyl hydrogen of Ser106 (O–H distance 2.57 Å). In summary, the electrostatic interaction of the PR groups of heme H_h is more symmetric than that of heme H_i. It is not accidentally that each PR pair belonging to the same heme at neutral pH carries in total one negative charge, since only one arginine per heme is involved in a salt bridge. In that way, the propionic and the corresponding arginine charges neutralize each other in low dielectric medium of the binding pocket.

The calculated isoelectric point of the native Cbc₁ complex is pI = 7.25. Since it is a transmembrane protein complex, which consists of predominantly hydrophobic residues, it is not surprising that its total charge is close to zero at neutral pH value. In contrast to the artificial Cb, the titration curve of the whole Cbc₁ complex (not shown) does not show a clear separation between acidic and basic residues. Since many of them are buried in low dielectric medium of the protein, their pK_a values can be considerably shifted from the solution pK_a values. There are also 57 histidines, which titrate at neutral pH. Thus, the action of all titratable residues together lead to a titration curve of whole protein complex that appears relatively smoothly.

6.2.2.2 *Experimental values of the heme redox potentials*

The complex III from respiratory and photosynthetic electron-transport chains have the universal redox center composition of two cytochrome b hemes, one cytochrome c heme (*c₁* of *f*), one Fe₂S₂ cluster, and up to one bound ubi- or plasto-quinone (Hurt & Hauska, 1981). Substoichiometric amounts of the Rieske Fe-S protein and of quinone (Weiss & Kolb, 1979; Engel et al., 1980) result from the use of Triton X-100 during the isolation procedure, what might be responsible for their partial loss. The redox potentials of hemes in native Cb differ considerably from the value in aqueous solution. With the preparation of Hatefi (1978) from bovine heart, two midpoint potentials were found (Table 6.2). The higher value corresponds to a component with an α -peak at 562 nm, the lower to a component with an α -peak at 565 nm plus a shoulder at 558 nm (Nelson & Gellerfors, 1974, 1975). The difference in redox potentials between low and high potential hemes is 127 mV. Both potentials are pH dependent in the physiological range (Von Jagow & Sebald, 1978; Von Jagow et al., 1981), being about 40 mV more negative at pH 8 compared to pH 7. After isolating the Cb from the complex, the spectral differences disappear, leaving only the α -peak at 560 nm, but the redox heterogeneity is retained with a considerable shift to lower midpotentials (-5 and -85 mV), which are still pH dependent (Von Jagow et al., 1978). The redox potential of the H_h heme in isolated Cb becomes 98 mV more negative, while the shift of redox potential of H_l heme is 51 mV, in comparison with their potentials within the Cbc₁ complex. It suggests that some conformational changes occur in the structure of the Cb. The individual values of the redox potentials of the Cb hemes vary for different species, as one can see from Table 6.2, for bovine heart and *Rhodobacter sphaeroides*. Due to the differences in the preparation procedure, the measured values of the redox potential can differ by 20 mV or even more. In comparison with the artificial Cb (Table 6.1), the closest values of the redox potential were found in the cytochrome b₆f complex from chloroplasts of plants (-50 and -170 mV), which is the functional analogue but non-homologue of the Cbc₁ complex.

6.2.2.3 *Calculated redox potentials in the whole Cbc₁ complex*

The calculated redox potentials of the hemes in the native Cb are displayed in Table 6.2, at three different pH values. They are considerably higher than the redox potential of heme in solution. The pH value of 6.6 was chosen for our computations, since the crystal structure of the Cbc₁ complex that we used was solved at that pH value. We calculated the redox potentials of the Cb hemes within the whole Cbc₁ complex assuming a solvent environment with a dielectric constant $\epsilon = 80$ outside of the protein complex. The calculated values of the

redox potentials deviate from the corresponding experimental values at pH 7 by 32 mV for H_h and 11 mV for H_l heme (32 mV is equivalent with about 1/2pK unit). The calculated values of the redox potentials for both hemes are more negative than the measured values, however they are still in a good agreement with experimental values, which are +93 and -34 mV for the high and low potential heme, respectively. Also the calculated difference of the redox potentials of two hemes correlates well with the experimental value (106 vs 127 mV at pH 7). In good agreement with experiments (Von Jagow et al., 1978; 1981) is also the pH dependence of the redox potentials, which decrease by 42 mV and 17 mV for the high and low potential hemes, at a pH between 7 to 8 (see Figure 6.2B). The strong pH dependence of the redox potential of the two Cb hemes arises from the strong coupling of the redox-active part of the hemes with the corresponding PR groups and arginines (Arg80, Arg100) involved in the salt bridges. Some other nearby titratable residues (His68, Lys227, Asp254) can also have a small influence. Since both hemes are well buried in the low dielectric medium of the hydrophobic pocket formed by the four-helix bundle, their electrostatic interactions with other charged groups in the protein are not screened by nearby aqueous solution, as it is partially the case for the artificial Cb. Consequently, their redox potentials are higher and their pH dependences are stronger than for the artificial Cb.

6.2.2.4 Calculated redox potentials of the hemes in the Cb subunit

Comparing the experimental data for the whole Cbc₁ complex and for the Cb subunit, one can see a considerable shift of the heme redox potentials to lower values. That shift is -98 mV for the H_h heme and -51 mV for the H_l heme. This difference in the behavior of the two hemes can be understood from the structure of the isolated Cb subunit (see Fig. 5.1), where the low potential heme remains well buried, whereas the high potential heme becomes more solvent exposed. Our calculated values show the same trend, where the isolation of the Cb from the protein complex causes a stronger decrease in the redox potential of the H_h heme. Namely, the computed redox potential of the H_h heme decreases by 26 mV, but the redox potential of the H_l heme is changed only by -7 mV. However, the obtained shifts toward the more negative values of the redox potentials are much smaller than in experiments. Furthermore, the calculated redox potentials are about 35 mV higher than the experimental values for the native Cb isolated from the Cbc₁ complex. This discrepancy is significant and may be due to differences between the conformation that the Cb subunit adopts in the crystal structure of the whole Cbc₁ complex that was used for the computations and the conformation that the native Cb isolated from the Cbc₁ complex assumes. On the other hand, the calculated difference of the redox potentials (87 mV) agrees very well with the corresponding experimental value for Cb isolated from the Cbc₁ complex (80 mV). Probably, in the structure of isolated Cb in a solution, both hemes are more solvent exposed than in the corresponding crystal structure of the Cb subunit. Hence, it is likely that some conformational changes occurs in the structure of the Cb if prepared in isolation. In agreement with experiments (Von Jagow et al., 1978), both redox potentials remain pH dependent, decreasing by 36 and 15 mV for the H_h and H_l heme, respectively, at pH between 7 and 8.

We also investigated the influence of the dielectric medium of the membrane on the heme redox potentials in the native Cb subunit. The membrane was modeled as a dielectric layer of 50 Å thickness with $\epsilon = 4$. The Cb subunit was embedded in the center of the layer, such that the normal of the layer was oriented parallel to the axis of the four-helix bundle. The obtained redox potentials at pH = 7 were increased by about 55 mV with respect to the calculated values in aqueous solution, with $\epsilon = 80$. We expect, however, that the influence of

the membrane is much smaller for the whole Cbc₁ complex, since then both hemes are well buried in the protein complex. Interestingly, in our computation the membrane does not effect the difference in the redox potentials (91 mV), which practically remains the same as in aqueous solution (87 mV).

The Cbc₁ complex and the dielectric medium of the membrane can be considered to have a similar influence on the isolated Cb subunit. Therefore, we tried to compare the redox potentials calculated using the membrane with the experimental values for the whole Cbc₁ complex. Interestingly, the agreement between the calculated redox potential of the H_h heme within the membrane and the experimentally measured value within the whole Cbc₁ complex at pH 7.0 is perfect (+91 vs +93 mV). But, at the same time, the redox potential of the H_l heme, for the Cb subunit in the membrane, is 34 mV higher than the corresponding experimental value in the whole Cbc₁ complex. Hence, this agreement of the calculated and measured redox potential for the H_h heme should not be taken too serious.

Table 6.2. Redox potentials of hemes in native Cb at different pH in mV

experimental values	high potential heme	low potential heme	difference
bovine heart mitochondrial cytochrome bc ₁ complex ^a	+93	-34	+127
Cb isolated from bovine heart cytochrome bc ₁ ^b	-5	-85	+80
Rhodobacter sphaeroides cytochrome bc ₁ complex ^c	+50	-60	+110
cytochrome b ₆ f from chloroplasts ^d	-50 -45	-170 -150	+120 +105
computed values from cytochrome bc₁ complex	at pH 6.6, 7.0, 8.0	at pH 6.6, 7.0, 8.0	at pH 6.6, 7.0, 8.0
whole complex in solution ($\epsilon = 80$)	+75, +61, +19	-37, -45, -62	+112, +106, +81
Cb from C chain only in solution ($\epsilon = 80$)	+46, +35, -1	-42, -52, -67	+88, +87, +66
Cb from C chain only embedded in membrane ^e	+106, +91, +42	+22, 0, -52	+84, +91, +94

^a Measured at pH = 7.0, (Nelson & Gellerfors, 1974).

^b Measured at pH = 7.0, (Von Jagow et al., 1978).

^c Measured at pH = 7.0, (Gabellini et al., 1982, 1983).

^d Measured at pH = 7.0; upper value (Hurt et al., 1982); lower value (Kramer & Crofts, 1994a,b).

^e A membrane of 50 Å thickness was assumed. Within the membrane, the dielectric constant was set to $\epsilon = 4$.

6.2.3 Redox titrations

The acid-basic titrations of ionizable groups in proteins have been widely investigated theoretically by using the continuum electrostatic method (Bashford & Karplus, 1990; Beroza et al., 1991; Yang et al., 1993; Antosiewicz et al., 1994; Beroza & Case, 1996; Lancaster et al., 1996). In some work, the redox potentials of the redox-active cofactors were considered (Gunner & Honig, 1991; Gunner et al., 1996; Muegge et al., 1996; Rabenstein et al., 1998a,b) or the pH dependence of the redox potential was studied (Beroza et al., 1995; Soares et al., 1997; Baptista et al., 1999). In most of these studies, the influence of the redox state on the protonation pattern was considered. However, the influence of the solvent redox potential on the oxidation and protonation pattern of variably charged groups in the protein was always neglected. An important aspect of the electrostatic computations, which I included in the consideration, is the possibility to perform a redox titration of a protein, by varying the external redox potential E_{sol} in eq. 2.47, and evaluating the corresponding protonation and oxidation probabilities of titratable groups by a Monte Carlo method. The solution potential was changed in 20 mV increments in the range from -400 to $+300$ mV. A similar approach was recently applied on cytochrome c_3 (Ullmann, 2000), however the probabilities were calculated by a hybrid statistical mechanics/Tanford Roxby method. In this section, some selected examples, which demonstrate very well the usefulness of the redox titration will be shown. The purpose of plots in figure 6.3 is to demonstrate which kind of information can be obtained from the simulated redox titrations.

Figure 6.3A displays redox titration curves of the two hemes in the artificial Cb at $\text{pH} = 7$ and $I = 0.1\text{M}$, where the oxidation probabilities of the redox-active groups are given as a function of the solution redox potential. The midpotentials ($E_{1/2}$) at $\text{pH} = 7$, that one can read from this plot, are -92 and -175 mV for the high and low potential heme, respectively. Due to the electrostatic coupling of the two hemes, these curves deviate from the standard behavior of an isolated uncoupled heme, whose titration behavior is defined by Nernst law. However, since the coupling of the two hemes in the artificial Cb is small (see section 6.2.1.4), this deviation is also small. Figure 6.3B shows the solution redox potential dependent E^0 value (defined by eq. 2.51) as solid line, and in addition the midpotential $E_{1/2}$ value (dashed line) for the same H_I heme, at $\text{pH} = 7$. The midpotential $E_{1/2}$ corresponds to the value of the solution redox potential at which the concentrations of the reduced and oxidized forms are equal. Interestingly, the potential of the H_I heme varies between -175.5 and -166.5 mV in the investigated range of the solvent potential, also indicating the small coupling (less than 10 mV) with the charged state of the other heme.

The influence of solution redox potential on titration behaviors of protonatable groups in artificial Cb is negligible. Since, the two hemes of native Cb are buried in a low dielectric environment and better shielded against the aqueous solution, their electrostatic coupling with the protonation reactions of titratable amino acid side chains is much stronger. Figure 6.3C displays the influence of solvent redox potential on changes of the protonation probabilities of some titratable groups in the native Cb, at $\text{pH} = 7$. As one can see, the protonation probability of the propionate PRA(H_h) attached to the high potential heme depends strongly on the solution redox potential. It decreases by 0.62 protons with oxidation of the corresponding heme. Other residues like PRD(H_I), Arg100, His68, Asp254, PRD(H_h) exhibit qualitatively a similar but weaker dependence. The so-called redox Bohr effect in the native Cb (Papa et al., 1979) seems to be associated with changes in the protonation states of charged residues with the oxidation of hemes, although the participating residues had not been experimentally identified. This plot may indicate that the coupling between hemes and these residues is responsible for the redox-Bohr effect in native Cbc₁ complex.

Finally, figure 6.3D displays the calculated population probabilities of the four different redox states of the native Cb at $\text{pH} = 7$, as a function of solution redox potential. The two letter

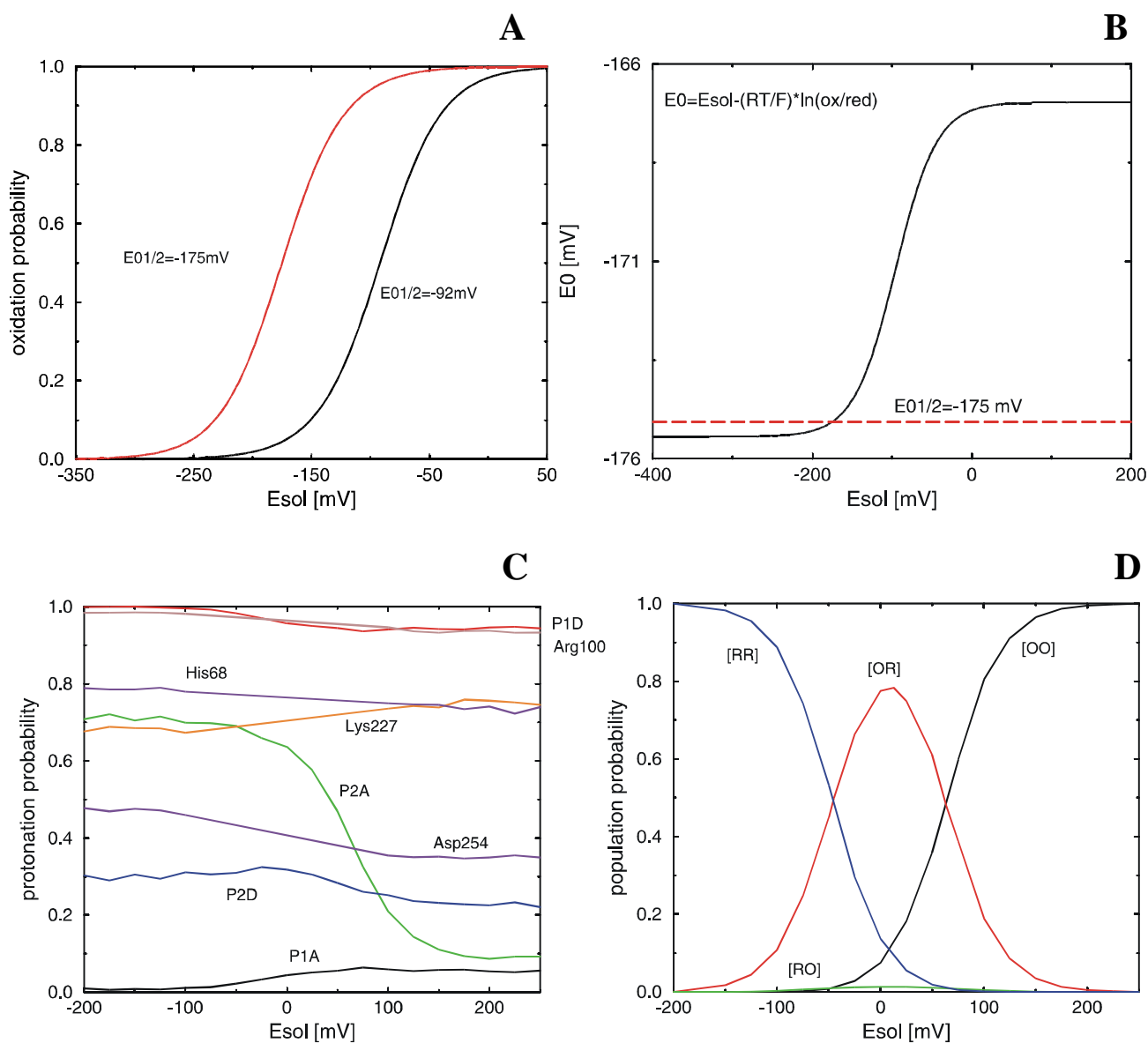


Figure 6.3: Selected examples that demonstrate how the results of the redox titrations can be used to obtain further informations. **(A)** Redox titration curves of the two hemes in the *artificial Cb* at pH = 7 and I = 0.1M. Redox titration curves of redox-active cofactors in proteins deviate more or less from the standard Nernst behavior, because of mutual coupling between each other. From this plot, one can read the midpotential $E_{1/2}$ values of the two hemes. **(B)** Comparison of the solution redox potential dependent E^0 value (solid line) and $E_{1/2}$ value (dashed line) for the H_1 heme of the *artificial Cb*, at pH = 7. This plot shows how much the actual value of redox potential deviates from the ideal Nernst behavior ($E_{1/2}$), due to the coupling with other titratable groups. **(C)** Dependence of the protonation probabilities of some titratable groups in the *native Cb* on the solution redox potential, at pH = 7. Displayed residues exhibit the largest changes of the protonation state in redox titration. That arises from the strong coupling between these ionizable residues and two redox-active hemes, whose oxidation probabilities are directly dependent on the solution redox potential. However, protonation probabilities of some ionizable residues can also depend indirectly on the E_{sol} value. **(D)** Population probabilities of all four redox states of the *native Cb* from bovin heart at pH = 7. At very negative values of the solution redox potential, both hemes are in reduced state [RR]. With increasing solution redox potential first the low potential heme is oxidized, populating the [OR] redox state more. At $E_{sol} = 0$ mV, [OR] becomes the most populated state with a probability of 0.80. Finally, also the high potential heme gets oxidized at higher values of solvent redox potential.

code is used to describe the particular redox state, where the first letter refers to the H_i heme and the second letter to the H_h heme. For energetic reasons, only three redox states are significantly populated. More discussion about the coupling of protonation and redox reactions in proteins, as well as, about the pH dependent pK_a values and the solution redox potential dependent E⁰ values, can also be found in sections 2.2.6 and 2.2.7.

6.3 Conclusions

Model building of an artificial protein with two hemes, recently synthesized, was performed. Its structure consists of a four helix-bundle and a cyclic decapeptide as template and mimics the central part of the native cytochrome b. Since, there is no X-ray structure available, the structural elements of the artificial protein were carefully assembled from scratch using all known structural informations available and avoiding strain as much as possible. The generation of atomic coordinates by modeling techniques, energy minimization and molecular dynamics was done by using the program CHARMM22. To test the stability and to validate the generated structure, molecular dynamic (MD) simulation was done. The obtained RMS deviations of atomic coordinates were compared with RMS deviations of coordinates from MD simulation of an appropriate native counterpart. For that purpose, we were choosing the native Cb from bovine heart, where an X-ray structure of 3.0 Å resolution is available from the PDB as 1BE3 entry. MD simulations of the artificial Cb exhibit RMS deviations (1.45 Å for all atoms), that are typical for very rigid proteins with known crystal structure. The results of MD simulation suggests that the modeled structure is stable and strain free. Since, the RMS deviations for the artificial protein are as small as the one of native Cb, we concluded that the structural stability and robustness of the artificial Cb is similar to the stability of the native Cb.

The second very important validation test for our computer-generated structure was the computation of the redox potential of its two hemes. We wanted to study the factors on which ET process depends on and to investigate the factors how the protein environment shifts the redox potential of heme from the value in aqueous solution. Therefore, the evaluation of the redox potentials is of the crucial importance. The successful computation of the redox potentials of the two hemes in the artificial Cb also suggests that the atomic coordinates generated by a modeling procedure are reliable. It is generally agreed that for native proteins a three-dimensional structure prediction does not work, since the association of different parts of the structure, sequentially connected by turns in a single polypeptide chain, includes many possibilities of the interfacial packing, which are difficult to predict (Betz et al., 1996, 1997). However, forming small peptides with defined secondary structure (helices) and their binding to predetermined positions of a cyclic template, offers the possibility of overcoming the unsolved protein folding problem. Furthermore, it opened to us the possibility to successfully generate its structure. Namely, the artificial Cb consists of the four helices, a cyclic template and two hemes. So, all together there are five separate polypeptide chains and two cofactors. The template is a cyclic decapeptide with a uniquely defined anti-parallel β-strand structure. A clear separation between the helical and linker parts enables the helices to maintain their secondary structure. Experimental data also suggest, that there is a high α-helical content in the structure (81%). Furthermore, the relative position and orientation of the helices with respect to each other is well defined by the template with its linker elements. There is a specific distribution of hydrophobic and hydrophilic residues along the helix axes, which defines the mutual orientation of the helices. Namely, the helices are oriented with hydrophobic faces toward the center of the four-helix bundle, while the hydrophilic sides are

solvent exposed. The sequences of the two pairs of identical helices *F* and *G* are especially adopted to host the two hemes. And even more than that, to orient the hemes along the helix axis by forming the salt bridges between the heme propionic groups and arginines. In the shielding helices *G*, two glycines were positioned at the same height as the ligating histidines in the binding helices *F*, to accommodate the bulky edges of the two hemes. All of that makes this artificial Cb a structurally well defined model system to generate its atomic coordinates from scratch by modeling procedures.

To test the atomic charges and the whole computational procedure for the evaluation of redox potentials in the heme-proteins, we applied our methodology also to the native Cbc₁ complex from bovine heart. The obtained results are in good agreement with experiments. However, the agreement was even better for the artificial Cb. This may be by chance. But also the isolation and preparation conditions for the Cbc₁ complex can have an influence on the redox potential measurements. Notice, that the content of the quinones and Rieske protein depends on these conditions and the measurements from different groups can vary by 20 mV or even more. Such problems do not appear for the artificial Cb. Although the atomic coordinates of the artificial Cb are subject to considerable uncertainties due to the modeling procedure, the coordinates of the crystal structure of the Cbc₁ complex obtained at 3.0 Å resolution may also be uncertain to some extent.

The analysis of the factors determining the shift and the difference in the redox potentials of the hemes in the artificial Cb gave the following results. (1) The electrostatic coupling of the redox potential of the hemes is relatively small (<10 mV). (2) A change of dielectric medium from aqueous solution ($\epsilon=80$) to the protein ($\epsilon=4$) causes about 45% of a total shift of the heme redox potentials, the rest 55% is due to the specific charge distribution in the artificial Cb. (3) The backbone charges contribute 50% to the total shift of the redox potentials but do not affect the difference of the redox potentials. (4) The charges of the hydrophilic residues contribute about 50% to the difference in redox potential of the hemes and at the same time they give rise of -20% to the total shift. (5) The charges of the salt bridges between arginines and propionic acids shift the redox potential of the high potential heme (located near to the template) more than the low potential heme. Thus, they participate about 50% to the difference and 33% to the overall shift in the redox potential. (6) The template and the inner hydrophobic side chain charges have only a minor influence on the difference and the shift of the heme redox potentials, but they render the hemes less solvent accessible.

We demonstrated that the atomic coordinates of this artificial protein can be generated by a careful, stepwise modeling procedure. However, to test that the procedure really works it would be helpful to solve its X-ray structure. The modeling protocol that we used here can provide a guideline how to generate atomic coordinates for similar artificial proteins. Continuation of this work, on similar systems is a promising task. The good agreement between calculated and measured redox potentials enables us to analyze the factors of the protein environment determining the shift in the redox potentials of the hemes. That opens new horizons to understand how the protein environment tunes redox potentials of cofactors, what is important for their function and how one can construct artificial proteins with prescribed redox potentials.